ASME Journal of Turbomachinery
Online journal at:
https://asmedigitalcollection.asme.org/turbomachinery

Judith R. Farman[1]
Whittle Laboratory,
University of Cambridge,
Cambridge CB3 0DY, UK
e-mail: jrf55@cam.ac.uk

Ivor J. Day
Whittle Laboratory,
University of Cambridge,
Cambridge CB3 0DY, UK

Tony M. J. Dickens
Whittle Laboratory,
University of Cambridge,
Cambridge CB3 0DY, UK

James V. Taylor
Whittle Laboratory,
University of Cambridge,
Cambridge CB3 0DY, UK

Zahid Hussain
Rolls-Royce plc,
Moor Lane,
Derby, DE24 9HY, UK

Compressor Water Extraction

The effect of putting a bleed slot behind the rotor or stator of a modern representative intermediate pressure compressor stage has been investigated using a purpose-built test rig. The first part of the paper goes over the construction and operation of a rig, which for the first time allows for accurate measurement of water extraction and rapid testing of a variety of bleed slot geometries. Using this test rig, it was found that the use of a bleed slot behind the rotor increases water extraction by up to 40 percentage points compared to placing it behind the stator. The overall extraction efficiency for the rotor exit was above 70% for all bleed rates considered from 0% to 30% and is relatively constant. Whilst rotor exit bleed might be advantageous for water extraction, further improvements in extraction efficiency are required for future engines with low fan speed and low blade solidity. The final part of the paper looks at the effect of a bleed lip protrusion to improve water extraction, as this can be retrofitted in engines. An extra 5 percentage points can be achieved by doing this without a penalty operability. This has been explained using 3D computational fluid dynamics by examining the flow separation topology. [DOI: 10.1115/1.4064419]

Keywords: compressor stall, and operability, bleed systems, computational fluid dynamics (CFD), measurement techniques

1 Introduction

Aircraft need to be able to fly safely through rain storms and the engines need to cope with water ingress without risk of flame out. The traditional method of removing water from the airstream in the core of the engine is to expel an air–water mix from a stator exit bleed slot in the compressor casing, out into the bypass flow. Such bleed slots have coped with the heaviest water ingress but further capabilities are being sought.

In most cases in the past, bleed slots have been positioned downstream of a stator row. This arrangement was favored because of the increase in discharge pressure derived from diffusion in the stator row.

With the idea of improving extraction efficiency, an alternative configuration, with the bleed slot downstream of a rotor row, is worthy of consideration—see Fig. 1. This configuration would make use of the natural tendency of water to be centrifuged radially outwards by the rotor blades. A boost in water extraction may thus be expected.

A novel study of the water extraction capabilities of a stator exit bleed slot versus a rotor exit bleed slot is reported in this paper. This work utilizes a functionally representative dynamic test rig.

1.1 Motivation. The design of modern engines favors an increase in bypass ratio, a reduction in fan speed, and a reduction in fan blade solidity. All three of these design trends increase the level of water ingestion into the core of the engine. Increasing levels of air bleed would improve water extraction from the core but it negatively impacts the cycle thermal efficiency. Future engines will therefore need improved water extraction efficiency, i.e., the quantity of water extracted for a given level of air bleed.

Rain is only one of the many reasons why water may be in the core of an engine. One source of water is from melted ice. As cold, moisture-laden, air passes over components and surfaces there is potential for ice accretion. This ice can then be shed and propagate downstream through the compressor. As the temperature rises through the compressor, the ice will melt with a risk of a sudden increase in the water fraction.

Too high a water content in the core compressors has three detrimental effects. First, it can stall the compressor as it mismatches. Second, it can cause damage to fragile blades as it increases loading. Finally, it can cause a flame out [1].

The worst conditions for water ingress into an engine occur during descent idle. In this phase of the flight, the engines are operating at low rotational speed as they descend through water-bearing clouds. To add to the complications of reduced engine speed and abundant water load, the effect of water scooping by the engine needs to be considered [2]. At low rotational speeds, the air-swallowing capacity of the engine decreases and some of the approaching air is forced to spill around the inlet. Rain droplets, on the other hand, do not spill around the inlet but follow a straight-line trajectory into the engine. This "scooping" effect tends to increase the concentration of water in the air entering the engine. Peak water extraction from the core thus needs to occur at near engine idle conditions, i.e., at low Reynolds numbers.

1.2 Possible Solutions. In the past, engine manufacturers have usually opted for bleed slots positioned downstream of a

[1]Corresponding author.

Contributed by International Gas Turbine Institute (IGTI) of ASME for publication in the Journal of Turbomachinery. Manuscript received September 21, 2023; final manuscript received December 6, 2023; published online January 29, 2024. Tech. Editor: David G. Bogard.

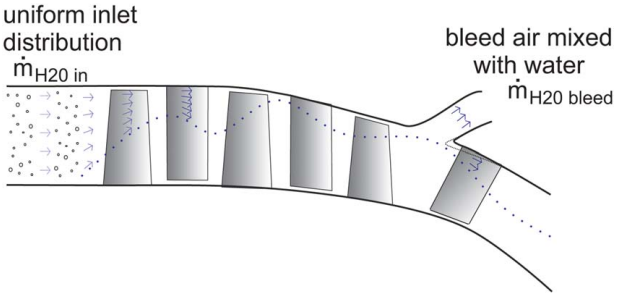

Fig. 1 Schematic of water distribution through the core compressor of an aero engine and its removal via the casing bleed slot

compressor stator row. Choosing this position utilizes the pressure rise in the stator row to increase the bleed pressure without extracting further work from the rotor. However, future engines will have larger bypass ratios with lower fan solidity and lower fan speeds and so will need a step improvement in water extraction.

Local modifications to the "stator exit" bleed slot could potentially be used to improve extraction efficiencies such as optimization of the following parameters: distance of the bleed slot downstream of the blade row, the radius of the leading edge of the slot, the width of the bleed slot, and the angle of the bleed slot relative to the casing and the casing line itself. Optimizing these parameters may not be sufficient and a more dramatic change may be required, however any new design needs to improve the water extraction without negatively impacting the performance of the engine.

The work by Day et al. [1] showed that, in the engine core, the inner 90% of the annulus is virtually dry. The rotor blade rows centrifuge any water content toward the casing and downstream of the rotor the water is concentrated in a sheet on the casing. The stator blade rows then redistribute a proportion of this water through the upper third of the span. An illustration of the distribution of the water across the blade rows can be seen in Fig. 1.

This work proposes the use of a "rotor exit" bleed slot as an alternative to the "stator exit" bleed slot in order to utilize the centrifugal effect of the rotor and the subsequent higher concentration of water near the casing. In a further development, it is proposed that the bleed slot trailing edge lip can be modified to penetrate into the main gas path in order to capture a higher proportion of the water content at the casing.

1.3 Literature Review. Experimental research by Murthy [3] was conducted on the propagation of water through a compressor on a single-stage low-pressure compressor as well as on a 2.5 pressure ratio axial flow compressor. He found that a film of water developed on the casing wall and there was a degradation of the compressor performance. Roumeliotis and Mathioudakis [4] investigated the impact of up to 2% water injection on a single-stage experimental compressor and found that the reduction in efficiency was proportional to the water ingestion. The research by Day et al. [1] investigated the distribution of water throughout a multistage compressor and found that water was centrifuged to the casing by the rotor blades and distributed across the span by the stator blades.

Significant research has been conducted on the optimization and effect of a stator exit bleed slot. For example, Grimshaw et al. [5] showed that non-uniform bleed caused by the number of off-take ducts and the plenum size can cause a circumferential distribution of flow coefficient and swirl angle at the downstream components. The research by Leishman et al. [6] showed that an axisymmetric slot downstream of a stator blade row in a region of nearly uniform static pressure caused no significant increase in loss.

Computational fluid dynamics (CFD) research by Saxena et al. [7] modeled a ten-stage high pressure compressor with bleed. The air bleed was modeled as mass source terms and it was found that stall-margin predictions could vary by as much as 25% depending on the droplet splash modeling. They concluded that experimental test data would be useful for improving the numerical models.

There is limited published research detailing the aerodynamic performance of a rotor exit bleed. A CFD study by Spanelis and Walker [8] on the use of a rotor exit bleed stated that the bleed effects were negligible on the aerodynamic performance below 25% of the mainstream flow. The CFD was validated with an experimental rig which lacked a bleed slot. Siggeirsson et al. [9] and Siggeirsson [10] detailed a CFD and experimental study for a rotor exit bleed but used a fixed pre-swirler to emulate the dynamic effects of the rotor. They found that an increased bleed rate caused an increase in incident swirl angle on the downstream components.

This is the first published work on two topics: experimental work on rotor exit bleed in a rotating rig, and the effect of bleed position and lip geometry on water extraction.

1.4 Approach. In this paper, the experimental study on a rotating compressor of these two modifications is presented. CFD simulations are used but only to explain the dry compressor performance trends and examine the separation topology. The focus is on obtaining previously unobtainable experimental data that can be used to validate future CFD studies.

First, the water extraction efficiency is compared for both stator exit and rotor exit bleed slot configurations. Second, the trailing edge lip of the bleed slot is varied in the rotor exit bleed configuration. The level of penetration of the bleed slot into the main gas path is varied in order to improve extraction efficiency.

2 Methodology

The majority of the work undertaken in this paper was experimental and involved the construction of a rotating compressor rig with representative hardware and a bleed extraction measurement unit with air and water flowrate measurement capability. CFD calculations were used only to support the dry measurement campaign.

2.1 Experimental Method. The research compressor is a one-and-a-half-stage compressor, representative of the rear stages of an intermediate pressure compressor similar to those proposed for future high bypass ratio engines. The compressor design parameters can be seen in Table 1. The test rig includes an additional stator blade row upstream of the rotor–stator blade rows under test. The upstream stator row is important for generating representative inflow conditions into the rotor blades, for both wet and dry conditions. In particular for the wet conditions, it redistributes the water film on the casing over the outer span of the compressor as illustrated in Fig. 1.

To simulate these conditions in the research compressor, water is injected onto the casing two chord lengths upstream of the first stator row. The water is injected at room temperature, i.e., less than 30 °C. The evaporation effects are not measured, are assumed to be small and therefore neglected. The water is injected tangentially, through an array of injectors at a velocity close to that of the rotor blade tips. The water fraction is controlled by the speed of the water pump and a diverter valve. The compressor velocity is kept at approximately the rotor tip blade speed by controlling the

Table 1 Design parameters

Rotor tip axial chord, c_R	(mm)	20
Rotor tip gap, τ	(% chord)	2.6
Tip inlet diameter	(m)	0.62
Hub-to-tip radius ratio	(–)	0.87
Rotor Re $= \rho_a V c_R/\mu$	(–)	7.4×10^4
Tip speed Mach number, M	(–)	0.16

pump delivery pressure and the number of injectors employed. The water fraction, R_{H_2O}, is defined as the ratio of the mass flow of water to the mass flow of air through the compressor.

$$\text{Water fraction: } R_{H_2O} = \frac{\dot{m}_{H_2O,inlet}}{\dot{m}_{air,inlet}} \quad (1)$$

A "complete flow conditioning gauze" (screen) is positioned upstream of the water injection location in order to produce representative inlet flow conditions to the first stator blade row. The gauze is printed in plastic and the design achieves the correct spanwise distribution of flow yaw angle and stagnation pressure by varying the turning and porosity distributions within the gauze itself, Ref. [11]. Figure 2 shows the target inlet conditions calculated from multistage CFD of a representative core. Alongside these are the predicted flow conditions from the gauze design CFD calculations. The short length-scale fluctuations are caused by the circumferential gauze blades, these are not expected to be present at the inlet to the compressor blade rows. In similar research compressors employing gauzes of similar designs the short length-scale fluctuations mix out completely within one span of the annulus [11].

The research compressor is speed controlled and under dry conditions can be tested up to much higher speeds than under wet conditions. A throttle is used to control the mass flow through the compressor, $\dot{m}_{air,\ inlet}$, and hence the flow coefficient, ϕ. At the design flow coefficient, at rated speed, the Reynolds number is 1.3×10^5. Due to limitations of the water pressure into the injector system, water fractions of 10% can only be achieved at 56% of the maximum compressor rotational speed. At this lower speed, the Reynolds number is 7.4×10^4. The Reynolds number is low compared to engine conditions, but it should be noted that at descent idle, the most critical speed for water extraction, compressor Reynolds numbers are also low. Rig performance in terms of its flow and pressure rise coefficients is measured via upstream pitot probes and casing static pressure tappings downstream of the compressor.

The compressor rig has been designed to test both a rotor exit and stator exit bleed slot. The geometries are plotted in Figs. 3(*a*) and 3(*b*) for comparison. The angle and radii of the bleed slot itself are not varied in this study but they are representative of a modern engine. The extraction efficiency is likely sensitive to the curvature of the casing line therefore it was deemed important to have a geometry similar to a real engine and to keep the casing line constant between the stator exit and rotor exit topologies. The rig components within the dotted box have been designed for rapid changeover to facility testing of multiple geometries.

With the intention of optimizing the water extraction capabilities of the rotor exit bleed slot, the bleed slot trailing edge lip was varied in terms of its protrusion into the flow stream— as illustrated in Fig. 4. The datum case maintains a smooth annulus line downstream from the rotor. The intermediate case extends the trailing edge lip into the annulus by 5%, this is blended out over the chord of the

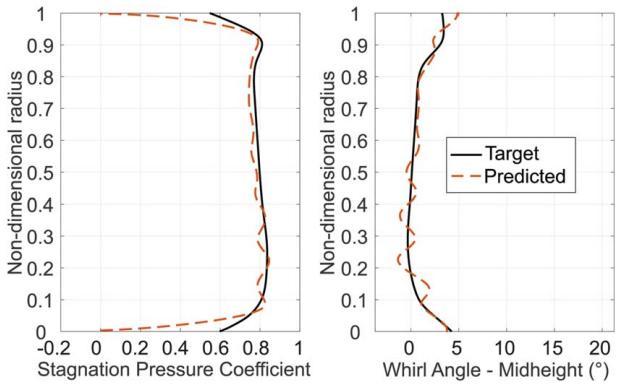

Fig. 2 CFD design of printed gauze to setup flow conditions ahead of first stator row

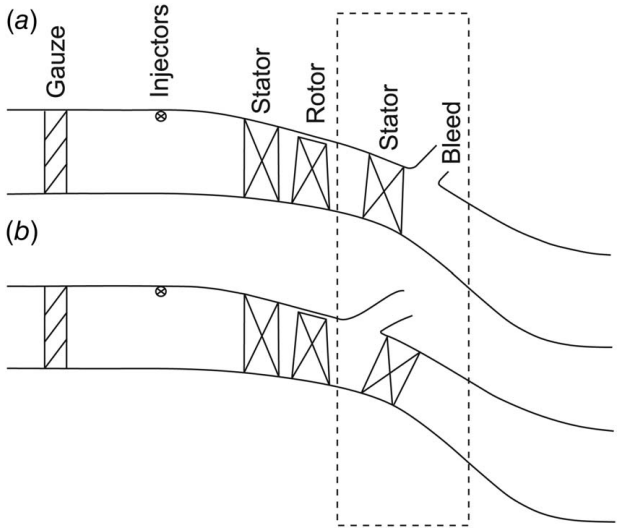

Fig. 3 Bleed slot positions: (*a*) stator exit bleed versus (*b*) rotor exit bleed

downstream stator blade. The extreme design penetrates 10% and is blended out over a longer axial distance.

In the test rig, the axisymmetric bleed slot dumps into the inter-casing region. The volume of this region is of the same proportions as in a typical engine. There are six off-take ducts from the inter-casing region at three circumferential locations and two axial positions. The purpose of these is to remove the air and water mixture from the inter-casing and deliver the mixture to the separator unit.

To measure water extraction efficiency and bleed rate in this experiment, the water–air mixture needs to be separated once it is removed from the inter-casing. The off-take ducts feed the bleed air–water mix through a unit which combines both a gravity separator and a drift eliminator. The water extracted, $\dot{m}_{H_2O,bleed}$, is measured by the height change of the water stored in a column by use of a pressure transducer placed at its base. The water extraction efficiency, η_{H_2O}, is the ratio of the water content removed by the bleed slot to the water injected into the compressor.

$$\text{Extraction efficiency: } \eta_{H_2O} = \frac{\dot{m}_{H_2O,bleed}}{\dot{m}_{H_2O,inlet}} \quad (2)$$

The dry bleed air then passes through an auxiliary downstream fan, via venturi flowmeters to determine the bleed mass flowrate,

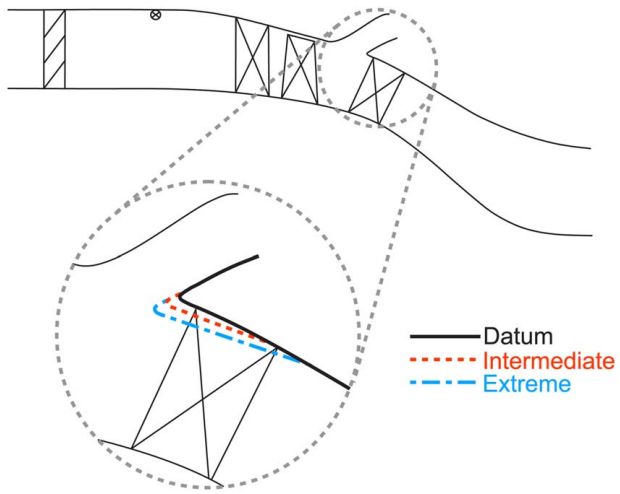

Fig. 4 Rotor exit bleed trailing edge lip profiles—datum, intermediate, and extreme

$\dot{m}_{\text{air, bleed}}$. The extraction fan is speed controlled to obtain the required bleed rate from the test compressor, R_{bleed}.

$$\text{Bleed air ratio: } R_{\text{bleed}} = \frac{\dot{m}_{\text{air, bleed}}}{\dot{m}_{\text{air, inlet}}} \tag{3}$$

2.2 Numerical Method. Modifications to the bleed slot geometry impact upon the compressor performance. CFD was run for the dry compressor configuration to support the experimental measurements and help interpret the results. Figure 5 shows the extent of the domain that has been meshed, mixing planes are placed between the three blade rows for the steady calculations. The second mixing plane is placed upstream of the bleed slot so that the correct three-dimensional potential field interaction and pumping with the downstream stator is captured.

The flow is solved using TURBOSTREAM [12] a second-order accurate graphics processing unit (GPU) accelerated, multi-block, structured, Reynolds-averaged Navier–Stokes code. One million cells are used in each passage, the walls are resolved to $y^+ = 1$, and the Spalart–Allmaras turbulence model is used [13]. The flow is solved to a steady-state with adaptive time stepping and multigrid acceleration. The grid is generated using AUTOGRID and utilizes a modern O-4H block topology, the tip gap of the rotor is fully meshed using a butterfly O-H block topology for minimum skewness. The bleed slot is fully meshed, however for the cases studied in this paper no net bleed flow is taken through the slot.

Constant speed characteristics are run for the three bleed slot lip geometries tested in the rotor exit bleed configuration. The solution is processed to calculate the total–total pressure rise coefficient and total–total efficiency of all three rows of the experimental test rig.

2.3 Test Campaign. The primary objective is to determine the efficacy of the bleed system design for removing water from the compressor. These tests were conducted at the design flow coefficient of the compressor for three water fractions 0%, 5%, and 10% and four bleed rates 0%, 5%, 15%, and 20%. These cover a representative range of operations in an engine.

Previous research showed that, for a multistage compressor with no bleed slot, there was a reduction in pressure rise and stall margin with increased water fraction. Consequently, tests were conducted on this research compressor to investigate the impact bleed has on the operating range under wet conditions. This work gives further information on different designs to enable an engineer to trade bleed system performance against compressor performance and operating range.

3 Experimental Findings

The results and discussion of the experimental work are presented in four sections. First, the dry performance of the compressor rig under a number of different bleed rates in both positions, stator exit, and rotor exit. Second, the measurements of water extraction efficiency for both bleed systems. Third, the sensitivity of water extraction to compressor rotational speed. Finally, investigations into different bleed slot trailing edge lip geometry, these include both experimental measurements of water extraction efficiency and CFD predictions of the dry compressor performance to show the major changes to compressor performance.

In this work, three variables are changed: water fraction injected into the front of the compressor, air bleed rate, and the geometry and location of the bleed slot itself. All of these three can impact upon compressor performance and operating range as well as water extraction efficiency.

3.1 Dry Performance. In this section of the paper, the characteristics of the compressor are presented for the bleed slots in both locations, with the datum geometry, under a range of bleed rates in dry conditions. The intention is to baseline the performance of the compressor before introducing the problem of water extraction.

Figure 6 shows a comparison of the measured compressor characteristics under a range of bleed conditions which have been nondimensionalized relative to the design flow coefficient and the peak pressure coefficient for the 0% bleed case. For the stator exit case, the conventional configuration, the bleed rate increases the performance across the entire range of operations. Choke margin is increased, as the casing boundary layer health is improved going into the downstream S-duct. With bleed the chance of separation from the casing side is reduced. Pressure rise at stall is also increased. At the high 15% and 30% levels of bleed, the flow is redistributed in the annulus enough to delay the separations that cause the characteristics to flatten out when flowrate is reduced below 0.9.

For the rotor exit case, it shows a similar behavior on the choke side, increased bleed improves the flow going into the casing end of the stator and the downstream S-duct. At the design point and near stall however there is an optimum bleed rate, with 5% bleed the maximum pressure rise from the stage is achieved. With the bleed slot in this configuration, the highest bleed rates could be interacting with the rotor.

The rotor exit case also has increased pressure rise relative to the stator exit case at all operating points. Note the changes in shape of the annulus and repositioning of the final stator in Fig. 3. Maximum pressure rise measured at the exit of the machine will depend upon the detailed flowfield in the final stator, but from these measurements, it seems that the rotor exit bleed configurations are beneficial for compressor performance.

3.2 Rotor Exit and Stator Exit Water Extraction. In most engines, the bleed slot is positioned downstream of a stator row. This benefits the bleed system efficiency as the stators recover pressure from the swirl component of the velocity at rotor exit in

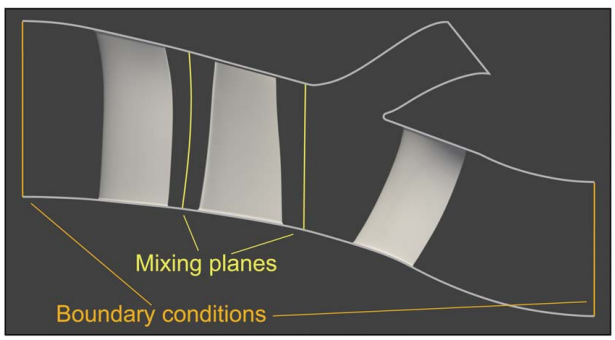

Fig. 5 CFD domain for rotor exit extraction with intermediate lip geometry

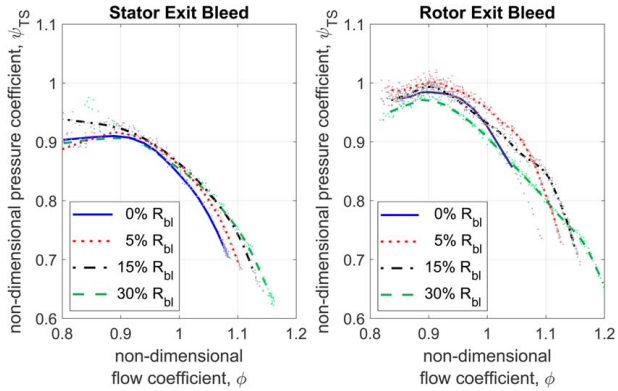

Fig. 6 Operating characteristics for stator and rotor exit bleed configurations at 0% water fraction

advance of the flow passing into the bleed slot. However, in future engines the problem of water extraction from the core will likely supersede this requirement. In this paper, bleed downstream of a rotor row is studied to take advantage of the favorable concentration of water on the compressor casing as shown in Fig. 1.

The water extraction efficiencies of the stator exit bleed slot and rotor exit bleed slot are shown in Figs. 7(*a*) and 7(*b*) respectively.

It can be seen that the stator exit bleed extraction efficiency depends on the bleed rate. This is most significant for the 2.5% and 5.0% water fraction condition which had an increase in the extraction efficiency of over 40% from 0% bleed to 30% bleed. At first glance, this may seem to be a useful trend, because the bleed rate can be increased if the water content is too high. However, in reality, the bleed system will not be able to achieve this due to other conflicting demands on the compressor.

Another trend in the stator exit bleed arrangement is the increase in extraction efficiency with water fraction. This is most pronounced at the 0% bleed condition, where the increase in extraction efficiency from 27% at 2.5% R_{H_2O} to 38% at 10% R_{H_2O} appears notable. However, since the intake mass flow of water has increased by a factor of four between these two cases, even with the greater extraction efficiency at the higher water fraction, the mass flow of water remaining in the engine's core has increased by a factor of 3.4.

The rotor exit bleed is significantly better at removing water from the core of the engine than the stator exit bleed, particularly at lower bleed rates. The lowest extraction efficiency was 63% at zero bleed for the 2.5% water fraction rather than 27% for the stator exit bleed at the same condition.

The rotor exit water extraction efficiency sensitivity to bleed rate was most significant for the 2.5% water fraction condition. For the other cases it is less, increasing by 8.5% and 6.6% with a bleed rate increase of 30%. On the whole, the rotor exit bleed configuration is four times less sensitive to bleed rate than the stator exit configuration. This means that the bleed rate cannot be used to increase the water extraction. However, as the minimum extraction efficiency is higher than that for the stator exit at almost all bleed rates, this is not considered to be a problem. Bleed rate will only be varied for normal operation such as startup bleed and cabin ventilation.

Day et al. [1] showed, for a compressor without a bleed slot, that an increase in the water fraction reduced the pressure coefficient and the operating range of the machine. In this work, these measurements are reproduced for the rotor exit bleed configuration including the effects of bleed. Figure 8 shows the measured characteristics which have been non-dimensionalized relative to the design flow coefficient and the peak pressure coefficient for the rotor exit 0% bleed and 0% water fraction case.

The 0% bleed case shows the same trends as Ref. [1], increasing water fraction from 0% to 5% and 10% reduces pressure rise at the design point and the flow range before the compressor stalls. However, taking bleed has a beneficial effect on the operating

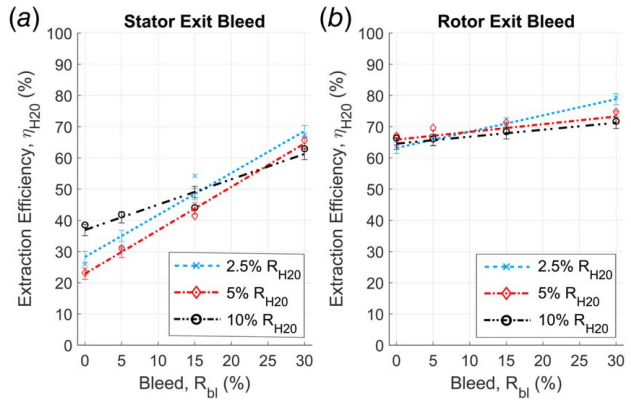

Fig. 7 Effect of bleed slot location on extraction efficiency ((*a*) stator exit bleed versus (*b*) rotor exit bleed) for three water fraction rates

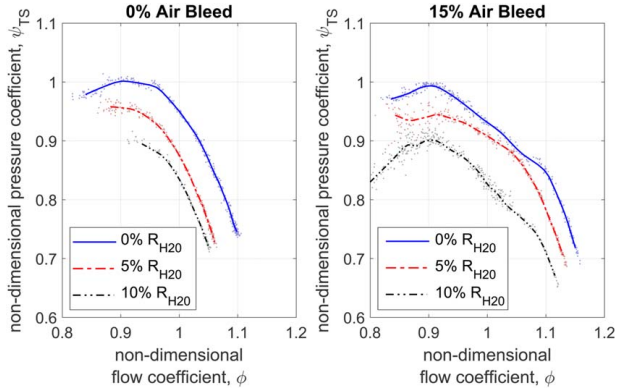

Fig. 8 Characteristics for datum rotor exit bleed

range of the compressor. With 15% bleed, the pressure rise at design is still reduced by a similar amount but the flow range is completely restored back to the levels of the dry compressor. This means that it is the presence of the water at the rear of the compressor that is most important at governing the flow range. Removing the majority of it with this efficient water extraction configuration removes the operability problem.

3.3 Sensitivity to Rotational Speed. The rotational speed of the research compressor is usually of little importance as the flow coefficient and pressure coefficient are non-dimensional. There are two reasons to test with it as high as possible, to keep the Reynolds number in the same regime as engine operation and to make the measurement signal-to-noise ratio as large as possible. On this rig, the speed of the research compressor was limited by the water injection system pressure. In order to achieve water fractions of 10%, the rotational speed in all previous results was set to 56% of the maximum compressor rotational speed. This section presents the results of a study where rotational speed was varied to investigate the sensitivity of the two bleed slot configurations.

Figure 9 shows, for both the stator and rotor exit bleed at 2.5% water fraction, that the extraction efficiency decreased with rotational speed. This has a proportionally larger impact upon the stator exit configuration. At 5% bleed, the water extraction is reduced by a third in absolute terms, while for the rotor exit configuration it is only reduced by a fifth.

This is the first time this effect has been reported and the impact it has on engine operation could be significant given that the absolute velocities in engine are higher even than the highest speeds tested on this rig. The mechanism must be driven by the distribution of water in the annulus and the positioning of the bleed slot relative to the rotor blade. At higher speeds, the water will be less favorably

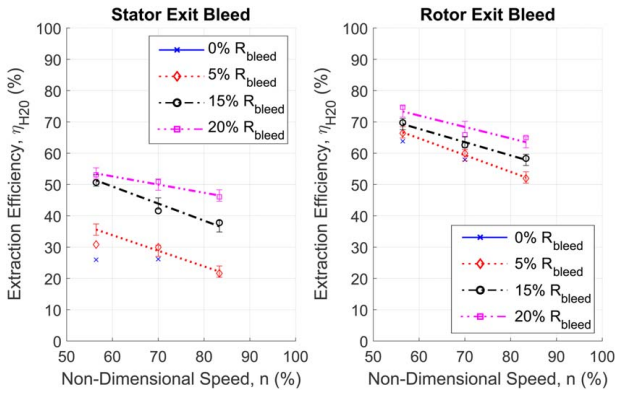

Fig. 9 Effect of rotational speed on extraction efficiency for 2.5% water fraction

distributed for extraction. At least, the negative effect of greater speed applies to both stator and rotor bleed off-takes and thus does not negate the improvement in water extraction efficiency observed for the rotor exit bleed slot.

3.4 Bleed Slot Geometry. The rotor exit bleed slot is more efficient at extracting water than the stator exit bleed slot, but there may still be improvements which can be made to the rotor exit bleed slot lip which will further improve its efficiency. The improvements investigated in this work concentrate on the penetration of the rotor bleed slot lip into the main airstream. The three configurations tested are shown in Fig. 4.

Figure 10 shows the extraction efficiency for the datum, intermediate, and extreme penetration lips. The results suggest that the optimum geometry for extraction efficiency is an intermediate lip, it was better than the datum by at least 1.8 percentage points for all bleed rates. The graph includes the error bars that are derived from repeat tests and rebuilds of the research compressor. As the improvements for these lip geometry changes have relatively small effects on the extraction efficiency, unlike the large-scale improvements for the move to rotor exit bleed, the statistical significance is reduced. Nonetheless, the performance improvement is particularly apparent for the 0% bleed condition which is where it is most beneficial.

The main issue with employing a lip which protrudes into the core flow is the potential for a deterioration in the compressor efficiency and performance. Figure 11 shows there is an increase in the overall pressure rise as the lip becomes more extreme, both at the design point and the maximum value that is achieved before the stall point of the rig. In order to understand the detailed aerodynamics that govern this effect, CFD was used to model the compressor characteristics, note that this was only possible at the dry condition.

Figure 12 shows the total–total pressure rise coefficient and the polytropic efficiency of the rig plotted against non-dimensional flow coefficient. At the design point, the total–total pressure rise is very similar for all lip geometries, this means that the change in pressure rise observed in Fig. 11 is an increase in casing static pressure only, the work output from the rotor is unaffected by the lip geometry. The small reduction in exit total pressure at design for intermediate and extreme lip designs can be attributed to a reduction in efficiency at the design point.

The surface limiting streamlines at the design point are plotted on the stator downstream of the rotor exit bleed slot in Fig. 13, the contours show stagnation pressure loss downstream of the stator. As the lip is moved into the passage the stagnation line moves further up into the bleed slot. At 0% bleed, this increases diffusion as the flow passes around the lip into the passage, reducing the health of the casing boundary layer. This increases the size of the casing

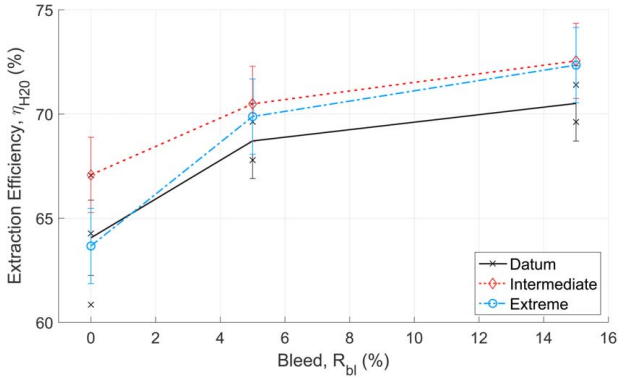

Fig. 10 Effect of trailing edge bleed slot design on extraction efficiency for datum, intermediate, and extreme lip designs

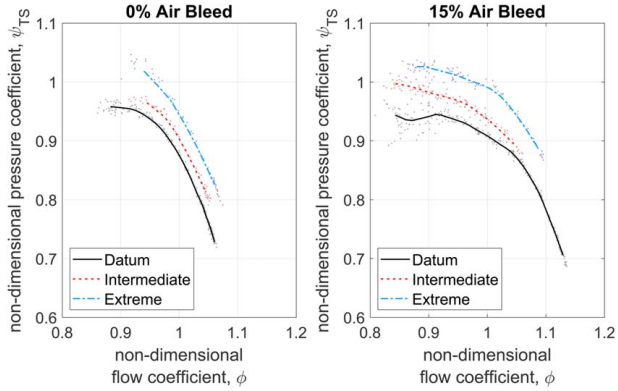

Fig. 11 Characteristics for rotor exit bleed with a trailing edge lip tested with 5% water fraction

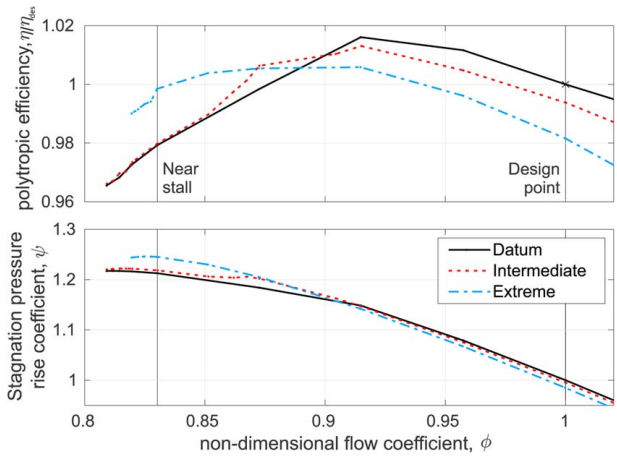

Fig. 12 CFD predicted dry characteristics at 0% air bleed

corner separation, and in the case of the extreme lip it reduces rig efficiency by 1.9% relative to the datum.

Near stall, the behavior switches and the extreme lip has better performance, efficiency is increased by 1.9% relative to the datum and the pressure rise is also higher. This is because both the intermediate and datum designs suffer from open-corner separations [14] at the hub when their flowrates are reduced to the critical values of 0.875 and 0.917 respectively. This can be seen in Fig. 14 where the surface streamlines show saddle points at the leading edges and increased losses downstream at the hub. The extreme lip has a closed-corner separation at the hub and is well balanced with the casing end, thus achieving the maximum operating range of the three designs tested.

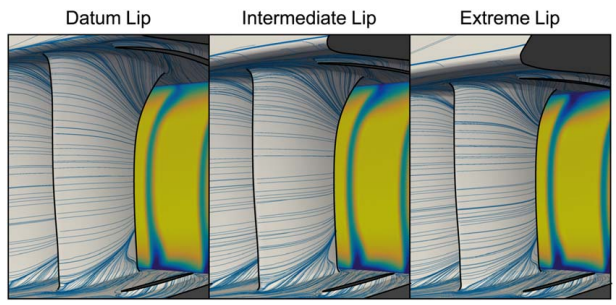

Fig. 13 CFD results for operation at the design point showing suction surface streamlines and stagnation pressure loss contours for datum, intermediate, and extreme lip designs

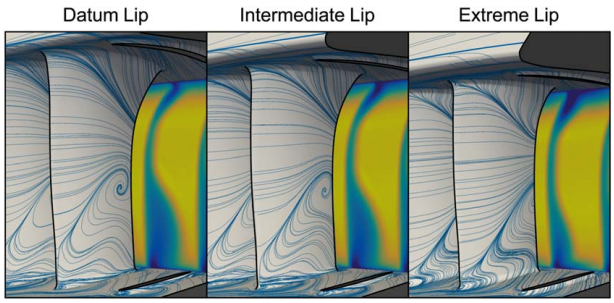

Fig. 14 CFD results for operation near stall showing suction surface streamlines and stagnation pressure loss contours for datum, intermediate, and extreme lip designs

4 Conclusion

In the pursuit of reduced fuel burn, some of the design choices being made result in an engine which is more susceptible to water ingress. The need to improve water extraction from the core is becoming ever more important. This water content needs to be removed as early on in the engine as possible to prevent aerodynamic, mechanical, and operational issues.

Tests were conducted on a rotating compressor with both the conventional stator exit bleed slot and a rotor exit bleed slot. The rotor exit bleed slot showed superior extraction efficiency for all bleed flow conditions. In particular, the rotor exit slot is very effective at water extraction at 0% bleed flow. Under 0% bleed flow conditions, the rotor exit design improved water extraction efficiency by 36% in comparison with the stator exit design, an improvement by a factor of 2.3. The superiority of the rotor exit slot over the stator exit slot can be explained by the known tendency for the rotor to centrifuge water onto the outer casing wall.

The water extraction efficiency for the stator exit bleed slot design was significantly dependent on the bleed rate with an increase of 40 percentage points between 0% and 30% bleed for the 2.5% water fraction case tested. The rotor exit bleed design however was significantly less dependent on the air bleed flow and had only a 16 percentage point increase for the same conditions.

The trailing edge lip of the rotor exit bleed slot was modified to penetrate into the main gas path in an attempt to improve the water extraction efficiency. Protruding by 5% into the gas path was better than a more extreme protrusion of 10%, it was also superior to the datum at all bleed rates tested. These results show that an optimal intermediate design is likely to exist.

The bleed slot lip design impacts upon compressor performance and shows that bleed system design must be undertaken simultaneously with the compressor design. The extreme bleed slot lip design had the largest pressure rise before stall as it beneficially affected the balance between hub and casing corner separations at these extreme operating points.

This work has shown that water extraction efficiency depends on both the geometry and flow conditions. Experimental test campaigns like this, that are representative of the real engine, are useful in understanding the propagation of two-phase flow through an engine due to current limitations of modeling.

Acknowledgment

The authors would like to thank Rolls-Royce Plc for their contribution to this work and to ATI/Innovate UK for funding the research (Project 113105). They are also grateful for the comments and suggestions of colleagues at the Whittle Laboratory and Rolls-Royce Plc. Most notably Geoff Jones, Ed Spalton, and Simon Read.

Conflict of Interest

There are no conflicts of interest.

Data Availability Statement

The authors attest that all data for this study are included in the paper.

Nomenclature

$\dot{m}$ = air mass flow (kg/s)
R_{H_2O} = water fraction (%)
R_{bleed} = air bleed rate (%)
η_{H_2O} = water extraction efficiency (%)

References

[1] Day, I., Williams, J., and Freeman, C., 2008, "Rain Ingestion in Axial Flow Compressors at Part Speed," ASME J. Turbomach., **130**(1), p. 011024.1.
[2] AGARD, 1995, "Recommended Practices for the Assessment of the Effects of Atmospheric Water Ingestion on the Performance and Operability of Gas Turbine Engines," Technical Report 332, AGARD, 7 Rue Ancelle, 92200 Neuilly-Sur-Seine, France.
[3] Murthy, S., 1996, "Effect of Atmospheric Water Ingestion on the Performance and Operability of Flight Gas Turbines," 32nd Joint Propulsion Conference and Exhibit, Lake Buena Vista, FL, July 1–3.
[4] Roumeliotis, I., and Mathioudakis, K., 2006, "Water Injection Effects on Compressor Stage Operation," ASME J. Eng. Gas Turbines Power, **129**(3), pp. 778–784.
[5] Grimshaw, S. D., Pullan, G., and Walker, T., 2015, "Bleed-Induced Distortion in Axial Compressors," ASME J. Turbomach., **137**(10), p. 101009.
[6] Leishman, B. A., Cumpsty, N. A., and Denton, J. D., 2006, "Effects of Inlet Ramp Surfaces on the Aerodynamic Behavior of Bleed Hole and Bleed Slot Off-Take Configurations," ASME J. Turbomach., **129**(4), pp. 659–668.
[7] Saxena, S., Woo, G. T. K., Singh, R., Breeze-Stringfellow, A., Nakano, T., and Szucs, P., 2016, "Effect of Ice and Blade Interaction Models on Compressor Stability," ASME J. Turbomach., **139**(4), p. 041001.
[8] Spanelis, A., and Walker, A. D., 2021, "Aerodynamic Influence of a Bleed on the Last Stage of a Low-Pressure Compressor and S-Duct," ASME J. Turbomach., **144**(2), p. 021007.
[9] Siggeirsson, E. M., Andersson, N., and Burak Olander, M., 2022, "Numerical and Experimental Aerodynamic Investigation of an S-Shaped Intermedidate Compressor Duct With Bleed," ASME J. Turbomach., **143**(10), p. 101003.
[10] Siggeirsson, E. M., 2020, "Aerodynamics of an Aeroengine Intermediate Compressor Duct: Effects from an Integrated Bleed System," Ph.D. thesis, Chalmers University of Technology, Gothenburg, Sweden.
[11] Taylor, J., 2019, "Complete Flow Conditioning Gauzes," Exp. Fluids, **60**(3), p. 35.
[12] Brandvik, T., and Pullan, G., 2010, "An Accelerated 3D Navier Stokes Solver for Flows in Turbomachines," ASME J. Turbomach., **133**(2), p. 021025.
[13] Spalart, P., and Allmaras, S., 1992, "A One-Equation Turbulence Model for Aerodynamic Flows," 30th Aerospace Sciences Meeting and Exhibit, Reno, NV, Jan. 6–9, AIAA.
[14] Taylor, J., and Miller, R., 2016, "Competing Three-Dimensional Mechanisms in Compressor Flows," ASME J. Turbomach., **139**(2), p. 021009.